Development of diagnosis & treatment technology for brain disease using quantum material and nano probe pin device.

Dr. Uhn Lee[1], M.D, Dr. Sang H. Choi[2], Dr. Vijay K. Varadan[3], Dr. Kyo D. Song[4], Dr. Yeonjoon Park[5]
[1]Gachon University of Medicine and Science, 1198 Guwol-Dong, Namdong-Gu, Incheon 405-760, Korea; [2]NASA Langley Research Center, Hampton, Virginia 23681-2199; [3]University of Arkansas, Fayetteville, AR 72701; [4]Norfolk State University, Norfolk, Virginia 23504; [5]George Washington University, Washington, D.C. 20052

ABSTRACT

New medical device technology is essential for diagnosing, monitoring, and curing wide spectrum of diseases, anomalies and inflictions. For neural applications, currently available devices are generally limited to either a curing or a probing function. In this paper we review the technology requirements for new neural probe and cure device technology currently under development. The concept of probe-pin device that integrates the probes for neurochemistry, neuroelectricity, temperature and pressure into a single embodiment with a wireless power transmission was designed for the purpose of deep brain feedback stimulation (DBFS) with insitu neural monitoring. The probe considered for monitoring neurochemistry is a microspectrometer. The feature and size of micro-spectrometer are defined for the DBFS device. Two types of wireless power transmission technology were studied for DBFS device operation. The test results of pig skin showed that both power transmission technologies demonstrated the feasibility of power feed through human tissue.

Keywords: neural probe, probe-pin device, wireless power feed, rectennas

1. INTRODUCTION

Recent advances in micro and nano-scale devices engineering and wireless power technology offer a great potential to revolutionize many health care systems. The integration of wireless power technology into smart microsensor and probe systems not only greatly simplifies the healthcare devices and systems, but also offers additional device functions for even complex jobs. The wireless power feed technology eliminates the pains and irritations associated with implanted power devices and wires. The News Feature of Nature magazine [1] clearly describes the benefit of deep brain stimulator (DBS). In its article, it mentioned about numerous DBS trials that has exploded since 1993, when Alim-Louis Benabid from the Grenoble University Hospital in France reported results from more than 80 patients with PD [2]. Around 30,000 similar operations have now been carried out worldwide with great success rate. It is sensational to see that a pulse of current through correctly placed electrode instantly stops the tremors and releases the frozen muscles which are characteristic of the disease. Neural electronics interfaces (NEI) can be coupled and integrated with the wireless power receiver (WPR). The implantable probepin devices (PPD) that include the NEI and WPR allow real-time measurement and control/feedback possible for remedial process of neural anomaly from normal functions.

*uhn@ghil.com; Phone 82 32 458 5020 Fax 82 32 458 5025

Nanosensors, Biosensors, and Info-Tech Sensors and Systems 2011,
edited by Vijay K. Varadan, Proc. of SPIE Vol. 7980, 798003
© 2011 SPIE · CCC code: 0277-786X/11/$18 · doi: 10.1117/12.880453

Such a system should have an embedded expert system that performs semi-autonomous functions through a routine of sensing, judging, and controlling the neural anomaly. This kind of devices require the expertise in areas of materials, microelectromechanical systems (MEMS), wireless networking, neurosciences and neurosurgery in general, motor and sensory control in particular. Over the years, pacemakers and defibrillators have saved millions of lives and revolutionized the cardiac care. Borrowing the pacemaker technology, surgeons now implant neurostimulators to control brain disorders. The implantable devices are also used to successfully block pain signals in the spine with pulses of electricity and effectively close the pain gate. Implantable devices are also used to control various pelvic muscles in patients with urinary and fecal incontinence. Even though the existing technology has tremendous impact on the control of the disease, it is still in infancy stage due to the use of wired network for power, data, and programming inside the human body. Certain symptoms of unusual physical behavior or psychiatric disorders are originated from brain malfunctions, such as Parkinson's disease (PD) and obsessive-compulsive disorder (OCD). People, such as the famous entrepreneur, Howard Hughes, a key character of a movie "The Aviator" suffered from OCD. People with OCD rarely go out because they fear contamination from anything they touch. An experimental surgical technique called deep brain stimulation (DBS) is currently the only hope for curing the OCD [1, 3]. The technique requires an implantation procedure of electrodes into deep brain to stimulate a certain portion of brain to function properly. It is not a new but already proved its value in the treatment of advanced PD. Neurosurgeons are now keen to try DBS to treat one of the world's biggest health burdens such as PD, OCD, and even major depression. Any treatment of these diseases using DBS involves the insertion of electrodes with probes incorporated deep in the brain to hit a precise neuroanatomical target that is believed to be central to the disease. The probes incorporated onto electrodes keep monitoring brain chemistry and neuro-electricity in a real time to maintain a functional feedback of brain. The electrodes of the conventional method used for PD treatment are connected to a battery-driven stimulator by a hard wire that sends pulses of current to the target neurons and normalized their activities, as shown in Fig. 1. The stimulator is sewn into the belly or chest for a known length of time it can sustain its function with the imbedded battery power. The connection between a stimulator and probe electrodes is networked by hard wires. The simulator can be switched on or off for probe functions at a remote distance. The wiring that runs from a stimulator to electrodes appears to be a quick solution for clinical trial, but it causes unbearable discomforts to a patient and is also often vulnerable to disconnection of the implanted wire under the skin. The disconnection of wire or power drainage requires repeated surgical procedures. Therefore, the technique to feed power wirelessly is great beneficial in clinical practice. The wireless power feed to the implanted electrode does not need any hard wire connection that otherwise has to run from a power source that is also implanted somewhere in the body. There are two different methods for wireless power feed to be adopted: The 1st method is the power generation by a magnetic induction coil (MIC). The power is generated when magnetic field lines of rotating magnets or alternating inductor current are cut by the implanted thin-film coils. The 2nd method is the thin-film rectenna array (TFRA) that receives incident microwave and convert it into DC power. The microwave rectenna technology developed at NASA Langley [4, 7] is used for harvesting microwave power that comes through the skin thickness. Research efforts for the development of wirelessly powered PPD by a multi-

disciplinary team of researchers are underway by solving the problems associated with today's Functional Electrical Stimulation (FES) for motor and sensory controls and NEI devices. By combining microelectronics and nanotechnology with BioMEMS and applying them at the cellular level for the development of a total wireless feedback control system, the implantable devices are wirelessly modularized.

2. TECHNOLOGY ROADMAP

2.1 Main Goal:

The aim of this paper is to *deliver* a complete wireless control of neural functionality that will alleviate neurally dysfunctional elements or enhance all functionality of weakened neural elements. The wireless control unit possesses a full sensory feedback component to understand and correct the monitored functional differences. The planned system encompasses two noticeable technologies: (1) The remote power feed and control by wireless microwave [4-9] and (2) the field-coupled inductors [10].

2.2 Critical Technical Barriers:

The challenge in developing these "extremely aggressive" wireless power transmission (WPT) devices is clearly noticeable when it is compared to the stimulator that is sewn into the belly or chest and can be switched on or off remotely through a wire buried under the skin. Initial barrier is the development of a simple and miniaturized bio-embeddable power transmission device that comprises of a transmitter and a receiver. In particular, the receiver is the one embedded and must be small and thin in size and at the same time provide a simple structure for an easy implantation. The power receiver receives an electromagnetic (EM) power wirelessly transmitted through the skin from a transmitter and coverts the EM power into a direct current (DC) that will be conveyed to a probe-pin (a combination of an electrode and probes). The feature of the probepin device (PPD) that will be embedded inside the brain will incorporate a number of sensory systems to monitor the neural functions of internal brain. The site-specific function of brain requires a precise amount of control signal and power. Accordingly, a mapping of site-specific power requirement of brain will determine a probe-pin device with specific sensing capabilities.

Once the PPD is imbedded at a specific site, it is activated with a very low voltage and at the same time it should monitor brain chemistry and neuro-electricity in a real time to maintain a functional feedback of brain. For any deviation or change in monitored data, the feedback routine of PPD triggers compensatory or recovery logic to control the power for DBS. The lookup table of database for signal deviation or change is developed in conjunction with patient's symptom or behavior. The development of site-specific PPD that is able to (1) capture power wirelessly for brain control, (2) at the same time feed the power and monitor brain functions, (3) transmit the monitored data wirelessly to a logic system located outside the human tissue, and (4) process sensor signals for any compensatory responses is a challenging task. Incorporation of sensors on a tiny electrode stem of a site-specific PPD is technically challenging issue and requires a longterm commitment.

2.3 Rationale, Specific Capabilities and its Uniqueness:

Currently, there are no sensory feedback systems available for DBS. A better approach to implement a neurally controlled upper extremity or OCD reactions is to use already proven cochlear as well as visual cortex implant technologies. Such an interface would give direct, instantaneous access to the information that involves stimulation and feedback controls. The nanotechnology solutions will physically restructure the neuronal network so that the signals can be efficiently coupled to a telemetry system to control PD or OCD effects in a real time mode. Unfortunately less expensive brain activity recordings such as scalp EEG, which represents common electrical activity of millions of neurons in the widespread area of the cortex, lacks the ability to provide necessary time-varying motor control signals to a body part. It is clear therefore that onsite intracranial recording of brain activity at the precise location of troublecause is necessary to control malfunctioning brain disorder effects that are normally appeared on a patient.

If there is an efficient PPD for NEI implemented in motor cortex of human brain, it could be possible to read and control human limbs which will help to restore motor of patients. The advancements of nanotechnology and its solutions in many health care applications are already proved that, it could be possible to restore vision for blind patients by interfacing external devices with human brain. The specific purpose of a PPD for NEI using nanotechnology and cultured neurites onto it after implanted is to monitor neural behavior and control unintended motion of body parts through wireless interface between the PPD and the hat system as shown in Fig. 2. The PPD for NEI will be implanted in the tiny pathways of the motor cortex and the faint signals from the electrode arrays will be read and directly coupled to the antenna on the probe system. The telemetry signals from this antenna will then couple to the hat system which detects the signal and analyzes the data with a look-up table to identify brain functions specifically tied up with motions of body. Then, a specifically designed algorithm will generate a counter signal that will be fed back to the PPD wirelessly to normalize the brain functions.

The hat system comprises of a small microwave horn that feeds a low power at a selected frequency of microwave through an imbedded thin-film rectenna array (TFRA). The dipole rectenna technology is mature and readily available for any practical use [4-9]. Figure 4 shows a wireless power receiver with a probe-pin device (PPD) is implanted for deep brain stimulation (DBS). The thin-film based wireless power receiver (microwave rectenna array) that is placed between the head skin tissue and skull couples with incident microwave field (Fig. 4) to generate power for PPD functions. The penetration depth of microwave through a skin tissue is estimated with the electrical conductivity of skin tissue. The sensor cluster of PPD as shown in Fig. 5 consists of various sensing heads, such as quantum-dots (QD) NEI for temperature, pressure, chemistry, and electric voltage measurements which might use a very small amount of power up to a few milli-watt. Accordingly, the power will be used mainly for DBS and telemetry functions. The hat system shown in Figs. 1 and 7 consists of a small power microwave injection horn with an oscillator and an analytical data logger circuit. The data logger receives a signal from PPD through the injection horn antenna at a designated frequency that is different from power feeding frequency. The data of brain signal is analyzed in real time basis to determine whether brain motor functions have any abnormality. The brain abnormality is checked by unusual jolting shock voltages or abruptly decaying signals. Once the brain abnormality is checked and verified, the data logger circuit triggers a microwave oscillator-amplifier chain immediately to send the

necessary microwave power to the rectenna array implanted under the skin. The power received by rectenna array is converted into DC power. The mode and power from the rectenna array are already tailored to stimulate the portion of brain directly.

3. FUNCTIONAL ELEMENTS OF WIRELESS PPD FOR DBS:

Development of a neurally controlled, wireless powered PPD should provide all functionality and possess a full sensory feedback component. Figures 7 and 8 illustrate the functional bases of wirelessly powered PPD concept. The electrical impulses generated from the brain will wirelessly fed into a specially designed algorithm that tells the PPD to convey a control signal to the brain that requires correction of motion. Real-time correction of the jolt of muscles can be done by the feedback error correction algorithm which will be developed specially for the present application. Embedded sensor network which will help to sense-or-feel, will read the brain chemical change and associated neuro-electricity variation that might be tied up with the movement information of body parts and will feed back to the brain using the above algorithm. Such a scenario is shown in Fig. 9 which describes schematically each functional element of all system. The vision is to develop wireless and nanotechnology solutions to NEI with neurite cultured probes. Only implantable device in this proposal is the PPD, and all necessary controllers are placed between the skull and head skin. The wireless power and logic control unit continuously communicates with the PPD's sensors and electrodes through tiny wires within the stem of PPD. The internal control logic circuit also communicates with the outside hat system which consists of a master logic circuit and power source and feeder. To achieve this goal, this proposal will concentrate on two core areas: (i) Nanotechnology solutions for implantable PPD devices and (ii) Wireless network interface with implantable devices and its power allocation.

3.1 Probe-Pin Device (PPD) with Nano-Neural Electronic Interface (NNEI): Development of a PPD with nanoscale sensors for neural applications is pursued for implantable electrodes to effectively transfer the signals from/to the brain as shown in Fig. 3. The stem of PPD is structurally made out of a polymer or a ceramic material that is physiologically adaptive. The stem has a built-in sensor array with wires imbedded along the length of stem for signal transmission. The design of the wireless neural probe at the tip of PPD to meet its own objective is described in Figs. 5 and 6. This involves the development of a tiny and slender embodiment of electrode that incorporates nanoscale sensors at the tip of a wireless implantable electrode as shown in Figs. 5 and 6. The PPD consists of three major components, such as an electrode pin covered with insulation coating from the top through the tip area, a wireless power receiver, and nanoscale sensor array. The tip of PPD is populated with an array of nanoscale sensors and is only exposed to the surrounding brain tissue. The materials of PPD are non-reactive and inert to body fluids. The electrode is made from insulation-coated gold wires imbedded within a PPD structure. The nano-scale sensors are built with quantum-dots (QD) of diameter less than 100 nm directly on the tip of quartz optical guide or carbon nanotubes (CNT) of diameter 20-50 nanometers that may be grown vertically at the tip of gold electrode or built with an array of

platinum rods. Otherwise, the QDs are anchored or immobilized at the tip of quartz fibers. The wireless power receivers considered for the PPD implementation are either a rectenna array for microwave power conversion or an inductive coupler that converts either electrical or magnetic field into DC power (see Figs. 3 and 6). The power tailored for DBS should have a capability running from 0 to ±10 volts and from 60 to 500 μsec pulse-width at least 200 Hz level. Neurites are induced and cultured to grow over QD array or grow in between the wires of CNT to achieve a good electrical connection between the probe and the surrounding neurons in the cortex region. The nanoscale array of sensors will open more signal pathways inside the brain that can effectively deliver control signal at the neuron level. Several functionalities of PPD as shown in Figs. 7, 8, and 9 are the measurements of neuro-chemistry, neuro-electricity, pressure and temperature, in addition to cortical surface recording and stimulation, multiple recording mechanisms exploring electrochemical and intracellular recording techniques in addition to extracellular recording, tissue engineering to integrate with nano-neural implants. The novel intimate neural-electrical interface can be developed to read surface potentials about 40 to 90 microns at the cortical surface using functionally specific QD array or *f-CNT* as well as nanowire synthesized probes as shown in Fig. 10. This feature is built on at the tip of field potential probe (see Figs. 7-9. In some figures, it is labeled as "sensor E".). This could measure high fidelity local signals such as action potentials at the nodes of ranviers of the axons in the topmost layer. The axons, particularly at the terminals in cortex layer I and II, are very thin, likely in submicron scale. The vertically aligned NNEI fabricated on patterned metal contact on biocompatible substrate can be envisioned as dendritic conducting wires extended from the electrical circuit to reach the proximity of the active spots (the nodes of ranvier) of axons. These axons form a 3D interdigitized interface which will be more effective to collect signals from the neurons in a similar fashion that neurons collect post-synaptic signals from all branched dendrites.

3.2 Wireless Control Feedback Logic: An array of sensors at the tip of PPD monitors brain activities by measuring the changes in neuro-chemistry and neuro-electricity. The signals from brain through a tiny electrode inserted into neuronal pathways in the motor cortex, a brain region where voluntary movement originates as electrical impulses, are fed into a specially designed algorithm that determines how much power is needed for motion correction. The primary motor cortex, a part of the brain that controls movement, has thousands of nerve cells. For each arm movement, thousands of motor cortical cells change their firing rate, and collectively, that signal, along with signals from other brain structures, like the basal ganglia and the cerebellum is routed through the spinal cord to the different muscle groups needed to generate the desired movement.

3.3 Hat Module: Two types of hat module are considered for wireless power applications. The one consists of a rotating magnet disk as shown in Fig. 6, wireless transceivers, demodulator and a miniature inductively coupled antenna to receive the control pulses from the PPD sensors and to deliver these feedback signal to the implantable PPD electrodes. The other consists of a tiny microwave horn transmitter (see Fig. 7) and otherwise the rests are the same as the hat system for magnetic induction coil. This could be possible using a magnetic induction coil (MIC) or inductively coupled antennas or a thin-film rectenna array (TFRA). As shown in Fig. 11, the hat module receives RF signal from the PPD sensor and demodulates the control signals using the microcontroller. It could be possible to embed all necessary commands into the microcontroller for modulation, demodulation and pulse generation.

4. GENERAL DESCRIPTION OF KEY COMPONENT TECHNOLOGIES

4.1 Wireless Power Transmission - Thin-Film Rectenna Array (TFRA):

The use of microwave power for power transmission is not new but was numerously demonstrated [4-8]. The rectenna array that receives and converts microwave into DC power brought forth with innovative power allocation and distribution (PAD) concept as reported previously [6]. It is essential to see power transmission through human body tissues. For test purpose, polyurethane films and pig skins were used to simulate human tissues. Specifically, the following issues should be addressed as: 1) to what extent microwave can transmit without causing any health concers; 2) how much human tissue tolerates specific absorption rates (SAR); 3) how many other different approaches will offer wireless power transmission for medical applications. With X-band (10 GHz), microwave transmission through a pig skin was tested with rectenna arrays located under pig skin. We also used various polyurethanes as other alternative skin materials under X-band microwave exposure. Transmission rate through various polyurethanes under the threshold limit value (TLV) measured in the experiment, and dielectric constant was calculated from this experiment data. It is also useful to measure specific absorption rates (SAR) of polyurethanes and transmission rates through polyurethanes as well as pork skin. The results were presented for power transmission rates under varying thickness of polyurethanes and effectiveness and efficiency of rectennas under the TLV of microwave power [11].

The dipole micro strips were fabricated on a flexible polyimide membrane with a rectifying circuit that is based on Schottky diodes, inductors, and capacitors. This microwave power source was used to test various rectenna array fabricated for various applications. Transmission capability of microwave power through various polyurethanes and pig skin was measured by determining voltage and current outputs of rectenna. The polyimide rectenna arrays were connected to a power measurement system that was located at the exterior of the anechoic chamber by means of a dual output BNC connector. The distances between the horn antenna and the rectenna arrays varied from 25 to175 cm. Figures 12 and 13 show the output voltage and current of the rectenna at distance between 25 to 175 cm from the horn, respectively. The rectenna was positioned to the vertical direction. The results of output show the output of 10 VDC and 2.5 mA from the polyimide rectenna at 25 cm away from the horn. The output voltage is reduced by $1/r^2$ rule as the distance is increased. However, the output current of the rectenna shows that there are no significant effects on output within the near-field. In terms of output power, Figure 14 shows a preferential output with approximately 25 mW/cm^2 at 9 and 10 GHz of frequency. The optimum output power at 10 GHz under the TLV [11] showed approximately 12 mW/cm^2 at 50 cm away from injection horn. Through selected thicknesses of polyurethane, the output voltages of a rectenna array at 100 cm from the horn were measured and plotted as shown in Fig. 15. The absorption coefficient of the microwave through polyurethane could be calculated based on the result. Figure 15 shows the output voltages measured through various polyurethanes at 100 cm from the injection horn. The output voltages of the rectenna through various polyurethanes were similar to the output without any intervening materials on various frequencies. However, at near 9 to 10.5 GHz ranges, the output voltages were significantly decreased as much as 50% for 2.5 cm thick polyurethane. Since the Threshold Limit Value (TLV)

for 10 GHz is approximately10 mW/cm2, the experiment was performed under the TLV level. Figure 16 shows the output voltages from a rectenna array through a pig skin (0.17 to 0.22 cm thickness) at various distances. The output voltages were decreased rapidly at the range of 9 to 10 GHz. The outputs powers captured by a rectenna array through a pig skin are shown in Fig. 19. It shows a significant attenuation of power over 10.5 GHz frequencies, but the transmission at the 9 to 10 GHz showes a preferential result. The transmission rate of the output voltages varied 8 to 43 %. The transmission rate of the output power varied from 3 % to 31 %. A maximum transmission rate of 31 % was achieved at 8.5 GHz while the transmission rate of 12% was achieved at 10 GHz. Figure 17 shows a comparison of microwave power transmission with and without a pig skin. The two different types of materials such as polyurethanes and pig skin used in simulation of human skin-tissues have tested with microwave power in ranges of 8 to 12.5 GHz. Absorption coefficients of those materials on various frequency ranges have measured. Based on the result of the experiment, the absorption coefficients of polyurethanes varies from 0.3 to 0.5 mm^{-1} while the α for the pig skin varies from 1.1 to 2.5 mm^{-1} along with the frequencies. Typically, the skin depth ($= 1/\alpha$) at 10 GHz is about 1.7 mm for the pig skin, while the polyurethane is about 2.5 mm. The result showed significant different absorption coefficients depends on materials or frequencies.

Therefore, microwave transmission through simulated human skins need to be carefully tested with various human skin tissue, muscle, and hairs in terms of TLV and SAR (specific absorption rate) of all parts. The experimental results show positive results for power transmission through the simulant skin-tissues using far-field microwave. For the hat-installed near-field microwave case, the capacitive coupling mechanism of microwave dominates the power transmission and is more favorable and effective than the farfield coupling.

Optional Power Modulator with Micro-Induction Coil (MIC):

Thin-film magnetic induction coils are another option to be developed to generate power for operation of PPD. An array of magnets rotates right above the implanted MIC. The field lines from a rotating magnet array cut through MIC and induce an electrical current within the line of MIC. The amount of power generation is largely dependent on the number of coil turns and angular velocity of rotating magnet array. The magnets in an array are permanent magnets placed on a circular disk. The power from a MIC is going to be an alternating current (AC). Accordingly, a rectifying circuit of the AC power is installed on a MIC disk for DC power conversion. Of course, the mode of power through the rectifying circuit will be determined by the functions of implanted PPD for DBS. The thin-film based MIC wireless power receiver that is placed between the head skin tissue and skull couples with rotating magnetic field (Fig. 6) to generate power for PPD functions. The rotating magnetic disc is one of the options. Instead, a patch of micro-coils which is similar to the induction coil plate in Fig. 6 can be used to generate a pulse train of magnetic field under a pulse modulated current feed. In the case when the induction coil couples with the pulse train of magnetic field, it generates a train of DC pulse. This pulse mode coupling device does not have any moving parts to run, but a pulse forming circuit which is advantageous over a rotating magnetic disc. Tiny induction coils, as shown in Fig. 18, can be used to capture power from pulse mode of magnetic field. The induction coils are embedded with rectifying diode circuit. RF or micro-wave from outside will generate induced current on MIC, then the current rectified, stored, and used.

Device Concepts for PPD AND NNEI: ***Invasive cortical recording***

So far most successful work in connecting brain and machine for movement control are based on the neural signals extracted from the primary motor (MI) cortex [12-13]. As shown in Fig. 19, needle-like microelectrode Arrays (MEAs) on the tip of PPD are implanted in the brain penetrating into the MI cortex to provide direct brain-machine interfaces (BMIs) for intracortical recordings from ensembles of neurons [**a video clip showing the insertion of MEA**]. Areas of tens of microns are exposed at the tip [14] or along the shaft as active electrodes to catch the local electrical signal.

4.2 Sensing Media – Quantum Dots

Fundamental criterion of material performance as sensing media is the excited state phenomena in materials that depict a bound-bound, a boundfree, or free-free transition. It is natural that excited states evolve with time as equilibrium is reestablished. The intrinsic features that determine excited level of materials are (1) the transport processes, such as energy transport and charge transport, (2) the localization processes for energy and charge, and (3) subsequent ionic displacement process which results from the energy localization. There are usually several alternative channels for dissipating energy without ion displacements. The localization process often accompanies the trapping or self-trapping of an exciton (energy) or of a hole followed by a capture of an electron (charge). It is a general case of a meso-scale domain when localized (or trapped) charge or energy could result from some local structure difference in a region of a solid, perhaps an impurity, a defect, a surface, and a fluctuation in topology.

In such a body structure, electron moves freely with an effective mass somewhat modified by coupling to lattice polarization. Or otherwise, the electron would be localized and self-trapped in a region strongly distorted by the electron itself through the electron-lattice coupling. These phenomena was predicted by Landau in 1932 [15] and verified by Kanzig in 1955 [16]. Freely moving electrons within a small domain of a QD whose curvature falls under a critical dimension close to its lattice constants undergo a momentum transition that might yield the Compton radiation. Or the localized electrons may behave as the plasmon undergoing plasma oscillation and radiative damping of the valence electrons. Whichever the principle is applied, quantum-dots obviously have great advantages of spectral flux density in a photonic transition over any other quantum structures of materials. That is why quantum-dots whose diameters are smaller than 100 nm are most effective during optical coupling process and qualified as excellent sensing media. Sensing media is attached at the end of fibers or needle probes and reacts with the brain chemistry. QD structure is favored due to its size and photo-chemical stability. Quantum dots (i.e, CdSe or CdTe) have numerous properties that make them attractive for optical detection. These include broad excitation and size-tunable photoluminescence (PL) spectra with narrow emission bandwidths (full width at half maximum of ~ 25-45 nm) that span the visible spectrum, allowing simultaneous excitation of several particle sizes at a single wavelength. QDs also have exceptional photochemical stability and relatively high quantum yields. Combined, these properties are unmatched in any available commercial fluorophore.

Chemical Sensor with QD Sensing Media

As discussed earlier, the outer surface of the quantum dots can modified to react with specific

target chemical elements. Therefore these QDs can work as chemical sensors. An optical / acoustic signal in Surface Evanescent Wave (SEW) and Surface Acoustic Wave (SAW) through an optical fiber / acoustic conduit measure the reflected wave from QD array which is interfaced with the target neurons and synapses When we attach specific RNA piece or protein piece on the quantum dot, they combine with special pair RNA or protein. Thus they change the overall mass. If we send the surface acoustic wave, the resonance peak shifts when the functionalized RNA or protein makes reaction and becomes heavier. This change of mass can be detected with SEW/SAW device [17].

Pressure Sensor with QD

Pressure sensor as shown in the right of Fig. 20 is made with QDs packed under a thin membrane. The dielectricity of QDs varies with the packing density. When pressure in brain increases, the membrane compresses the QDs underneath and causes the change in dielectric constant. The charge imposed on QDs is applied between the center column electrode and the membrane with side column electrode. The capacitance value of membrane is affected by pressure on it. We will fill the gap of membrane with functionalized quantum dots in order to give elastic properties to the membrane as shown in the right picture of Fig. 20. This method can increase the sensing pressure range and recoil force of the membrane.

Temperature Sensor with multilayered structure and QDs

Temperature sensitive multilayer and QDs are attached on the tip-end of PPD as shown in the left picture of Fig. 20. Quantum dots have well-defined energy bands. These energy levels are sensitive to the ambient temperature. For example, quantum-dot optical temperature probes were developed using (CdSe)ZnS by Glen, W. W. et al.[18].

Voltage Sensor with QD

Nano-electrodes are fabricated with their own end-tips populated with the built-in QD as shown in the middle of Fig. 20. That is, QD are populated and attached on the tip-end of PPD. The QDs at the tip receive voltage signals from neurons and synapses. QD sensors attached on electrodes create a nano-circuit for terminal interconnection to neurons and synapses at inter-cellular and extra-cellular level. Time-resolved data sampling is performed on neural signals. The electric interface between quantum dot and neuron was first explored by Gomez, N., Winter J. O., Shieh, F., et al.[19] and Quantum Cellular Neural Network (QCNN) was studied by Qiao, B., Ruda, H.E. [20]. Our approach uses regularly controlled nano-electrodes driven from functionalized quantum dots. Eventually, we try to establish complex mathematical models based on these measurements.

4.3 Transducers:

The quantum-dots (QDs) anchored on a sensing head are highly sensitive and respond spectrally according to the surroundings. QDs have fairly broad excitation spectra that can be tuned depending on their size and composition and at the same time narrow emission spectra, making it possible to resolve the emissions of different nanoparticles simultaneously and with minimal overlap. QDs are highly resistant to degradation and readily functionalized for immobilization to a specific site of living tissues. Functionalized QDs are specifically attached to cells, proteins, and nucleic acids as powerful tagging agents. Accordingly, QDs anchored on a

sensing head can be also directly attached to living tissues on the other side of QDs. In such an arrangement, the changing environment in living tissues alters the signal response of QDs beyond the size and composition. The change or shift in emission spectra reflects the environmental alteration due to the change in metabolism or biochemical balances. Nanoshells (NSs) can enhance chemical sensing by as much as 10 billion times which is interpreted as about 10,000 times more effective at Raman scattering than traditional methods. Scientists at the Nanophotonics laboratory of Rice University found that nanoshells are extremely effective at magnifying the Raman signature of molecules. The candidate sensor technology is based on the QDs and nanoshells that are used as bioreceptor/transducer. At the tip of an optical fiber, a population of QDs or nanoshells all anchored on the surface perpendicular to the optical axis will interfaces with the element of living tissues, respectively one-to-one basis. The light transmitted through optical fiber excites QDs or NSs at the tip surface of fiber (see Fig. 21). The emission spectra from QDs or NSs are tailored by not only the size and composition of QDs or nanoshells, but also living tissues attached on QDs or nanoshells. The applications of gold nanoshells also include cancer diagnosis, cancer therapy, diagnosis and testing for protein associated with Alzheimer's disease.

4.4 Micro Ring Spectrometer

A team at NASA Langley Research Center developed a tiny micro-ring grating device [21]. Ray of concentric rings can be used a micro-ring grating. Tiny photon detector is located at separate distance with stray-beam blocking layer. The wavelength of the collected light will be selected by applied voltages on electro-optic media on the rings. Fabricated device and measured optical property are shown in Fig. 22. The working principle is shown in Fig. 23. Spectrometer is an optical device based on optical diffraction phenomena to separate the photons according to its wavelength. Diffraction of photons is typically described by either of Fraunhofer equation or Fresnel equation. Fresnel diffraction-based micro-spectrometer has about $1mm^3$ of optical volume between grating and photo-detector. This 1/1000 miniaturization of spectrometer optical components volume is possible due to utilization of Fresnel diffraction equation. Ultra-small miniaturization of spectrometer opens new opportunities including tiny medical optic instruments that can be embedded into human body. Ultra-small ring-shaped circular grating was fabricated on gold coated quartz substrate using gallium focused ion beam (FIB) with assistance of xenon difluoride (XeF_2) etching gas as shown in Fig. 22. The diameter of circular grating was 750μm with focal distance of 2.4mm for photons of 532nm wavelength. This design has 50 transparent rings and 50 opaque rings which are based half transparent Fresnel zone plate arrangement. Circular micro ring grating separates photons according to their wavelengths on the optical axis as shown in Fig. 24. The light enters circular grating and focuses on different points on the optical axis at specific optical distances. In Fresnel diffraction, the photons with shorter wavelength have larger optical distances. By moving the aperture slit on the optical axis, only the focused photons with desired wavelength can pass the aperture slit and enter the photon detector.

Otherwise, a electro-optical material behind the micro ring grating can focus the selected wavelength at the aperture slit by controlling the refractive index. Theoretical and experimental results are given in Fig. 25. Figure 25(a) shows mathematical simulation of calculated photon intensities of three different wavelengths, red line = 633nm, green line = 532nm, blue line = 450nm. Focal point F separates photons most, but higher order points such as F/3 shows axial

color dispersion as well. For experiment, a pseudo yellow light was made by mixing two lasers, green (532nm) and red (630nm) as shown in inset picture of Fig. 25(b). The mixed light was analyzed by micro-spectrometer which resolved two clear peaks at 532nm and 630 nm as shown in Fig. 25(b).

To the contrary, the resolving power of Fresnel diffraction spectrometer does not decrease as long as the same numbers of rings are maintained during miniaturization process [21]. The circular grating is not a simple lens but a circular arrangement of diffraction points. In the detailed Fresnel diffraction calculation, the spectral resolving power of Fresnel spectrometer is determined not by the grating size, but by the number of grating rings. Figure 26 shows the result of mathmatical simulation with various phase errors. The small dotted green line indicates photon distribution of half transparent circular grating. The solid green line shows the intensity from full transparent grating without phase error. While the quartz step height is optimized for 532nm with perfect phase matching, other wavelengths develop small phase errors such that solid blue line is intensity distribution of 450nm photons with +30% phase error and solid red line is the intensity distribution of 630nm photons with -20% phase error. As shown in Fig. 26, full transparent grating has upto 4 times of stronger intensity with much higher light collection efficiency compared with half transparent grating. With phase error the peak position does not change much but peak height drops relaltively. This indicates the sensitivity of Fresnel grating drops as the wavelength deviates from optimized λ. However within the visible spectrum the sentivity drop is minimal as shown in Fig. 26. More severe deviation such as $\pm$50% phase error is also simulated and plotted as dashed blue and red lines in Fig. 26. Therefore, we conclude that full transparent Fresnel grating gives much higher light collection efficinecy upto 400% for optimized wavelength compared with half transparent zone plate grating. Also phase matching error due to finite step height difference induced sensitivity drop as wavelength deviates, but still micro-spectrometer can cover full visible wavelength range.

The size of actual implantable PPD is very small in diameter up to 1.5 mm, with a tailorable length. Within the embodiment of PPD, there are several sensors mentioned above to be integrated for the real-time measurements or monitoring of neuro-electricity, neuro-chemistry, pressure, and temperature. These sensors must be built within nano or micro-scale level with reasonable sensitivity and responsivity to be integrated together without exceeding a form factor of 1.5 mm diameter. Micro-spectrometer was initially developed for NASA's future space exploration as shown in Fig. 27. Miniaturization capability of Fresnel-based micro-spectrometer has offered new medical applications, especially as a neural probe.

5. CONCLUDING REMARKS

Neural probe under development is very complex system that embodies several tiny sensors for monitoring neuro-electricity, neuro-chemistry, pressure, and temperature in a real-time basis with the capabilities of wireless power transmission and data telemetry. Development of sensors themselves poise great challenges to overcome the issues related to the sensitivity and responsivity at the nano-scale level, the refreshment of sensor interface with target tissue, and the physiological adaptability. Moreover, the wireless exchange capabilities of power and data telecommunication through human tissue are still remained to be fully answered and studied further although the research works to date have pulled new crossbred talents and technologies to

fulfill the objectives of PPD-like probe technology. Based on the progresses made so far, the realization of the PPD-like probe and instrument technology is not far away for clinical applications, owing mainly to the nascent nano- and bio-technologies. For an electrode of PPD that conveys suppression voltage as a response to neurally monitored anomaly jolt, a wireless power with logic circuit is able to handle the required functions. However, an eventual implantable PPD as a full-scale model requires that the responsive suppression voltage is programmed with the monitored results of neuro-chemistry on dopamine and serotonin, pressure, and temperature. Accordingly, an organized effort can answer all these issues for the development of PPD-like probes. We now see that such organized activities are underway with the reasonable level of supports all over the world. It is a reckoning moment to observe new developments and progresses through the acumen and scrutiny of the open domain of this journal.

AKNOWLEDGEMENT

This work was partially supported under the collaboration term between Gacheon University of Science and Technology and NASA (Space Act Agreement #15546).

REFERENCES

[1] New Feature, 7 July 2005, “Deep In Thought”, Nature 436, pp. 18-19.
[2] Benabid, A. L. et al., 1993, Acta Neurochir. Suppl. 58, pp. 39-44.
[3] Greenberg, B. D., Rauch, S. L., and Haber, S. N., 2010, "Invasive Circuitry-Based Neurotherapeutics: Stereotactic Ablation and Deep Brain Stimulation for OCD**",** Neuropsychopharmacology Review Journal, 35 (1), pp. 317-336.
[4] Choi, S. H., Kim, J. H., and Song, K. D., 2008, “Microwave Rectenna based Planarity Monitoring Sensor,” Korean Patent No. 10-0835924, June 2, 2008. U.S. Patent Pending No. 12/294,048, September 23, 2008.
[5] Kim, J. H., Yang, S. Y., Song, K. D., Jones, S., and Choi, S. H., 2006, “Performance Characterization of Flexible Dipole Rectennas for Smart Actuators”, IOP Journal of Smart Materials and Structures, Vol. 15, pp. 809-815.
[6] Choi, S. H., Golembiewski, W. T., and Song, K. D., 2000, “Networked Array Circuitry for Power Allocation and Distribution (PAD)”, Invention Disclosure, NASA Case No. LAR-16136-1-CU.
[7] Choi, S. H., Song, K. D., Golembiewski, W. G., Chu, S. H., and King, G. C., 2004, “Microwave Power for Smart Material Actuators”, IOP Journal of Smart Materials and Structures, Vol. 13, No. 1, pp. 38-48.
[8] Song, K. D., Yi, W. J., Chu, S. H., and Choi, S. H., 2003, “Microwave Driven Thunder Materials” Microwave and Optical Technology Letters, Vol. 36, No. 5, pp. 331-333.
[9] Lee, U., and Choi, S. H., 2008, “Sensory Control Using Neural Electronic Implants with

Microwave Wireless Power Feed", Patent Pending: PCT/KR2008/002662.
[10] Lee, U., Choi, S. H., and Park, Y., 2008, "Deep Brain Stimulation Device Having Wireless Power Feeding By Magnetic Induction", Patent Pending: PCT/KR2008/002664.
[11] ANSI C95-1992," American National Standard Safety levels with respect to human exposure to radio frequency electromagnetic fields, 300kHz to 100 GHz," New York; IEEE.
[12] Igor L. M., Tetsuo H. U., Ellen R. G., and Hedi, M., 2004, "Quantum dot bioconjugates for imaging, labelling and sensing", Nature Materials, Vol. 4., pp. 435-446.
[13] Donoghue, J. P., 2002, "Connecting cortex to machines: recent advances in brain interfaces". Nature Neuroscience Supplement, 5, pp. 1085-8.
[14] Moxon, K. A., Chapin, J. K., 1999, "Cortico-thalamic interactions in response to whisker stimulation in a computer model of the rat barrel system", Neurocomputing, 26-27, pp. 809-822.
[15] Landau, L. D., and Lifshitz, E. M., 1972, Course of Theoretical Physics: Physical Kinetics, Pergamon Press.
[16] Kanzig. W., 1955, Physics Review, 99, pp.1890.
[17] Jayarajah, C. N. and Thompson, M., 2002, "Signaling of transcriptional chemistry in the online detection format", Biosensors & Bioelectronics 17 (3): pp. 159-171.
[18] Glen, W. W., Vikram, C. S., Christina, M. R., Aetana, W. W., Moungi, G. B., and Daniel, G. N., 2003, "Quantum-dot optical temperature probes", Applied Physics Letters, Vol. 83 (17), p.3555.
[19] Gomez, N., Winter, J. O., Shieh, F., et al., 2005, "Challenges in quantum dot-neuron active interfacing", TALANTA 67 (3), pp. 462-471.
[20] Qiao, B. and Ruda, H. E., 1999, "Evolution of a two-dimensional quantum cellular neural network driven by an external field", Journal Of Applied Physics 85 (5): pp. 2952-2961.
[21] Park, Y., Koch, L., Song, K. D., Park, S. J., King, G. C., and Choi, S. H., 2008, *J. Opt. A: Pure Appl. Opt.* **10,** 095301
[22] Hirsch, L. R., Jackson, J. B., Lee, A., Halas, N. J., and West, J. L., 2003, "A whole blood immunoassay using gold nanoshells." Anal Chem 2003, 75, pp. 2377-2381.
[23] Kitaura. N., Ogata, S., and Mori, Y., 1995, *Opt. Eng.* **34,** pp. 584–588.

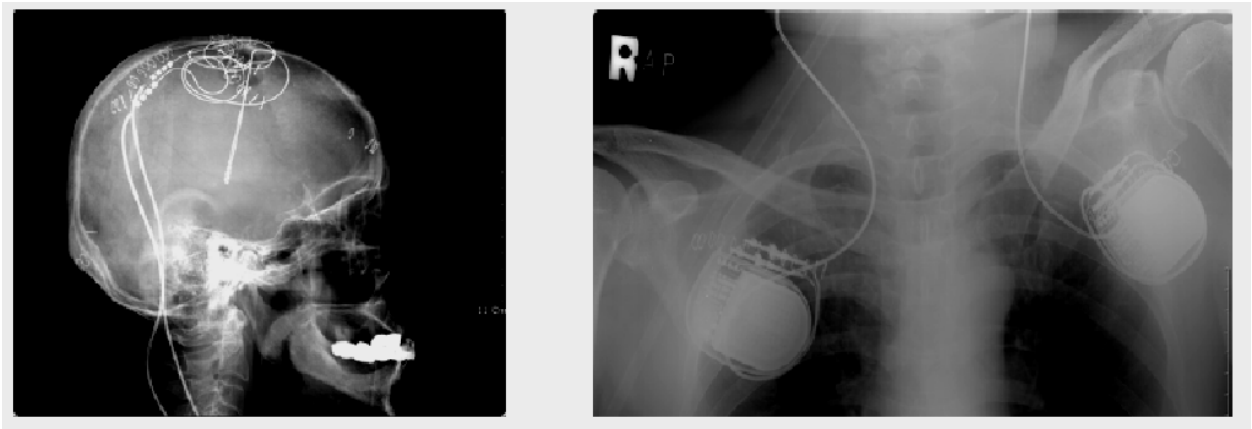

Figure 1. An electrode and batteries for DBS controlling the motor action of a PD patient.

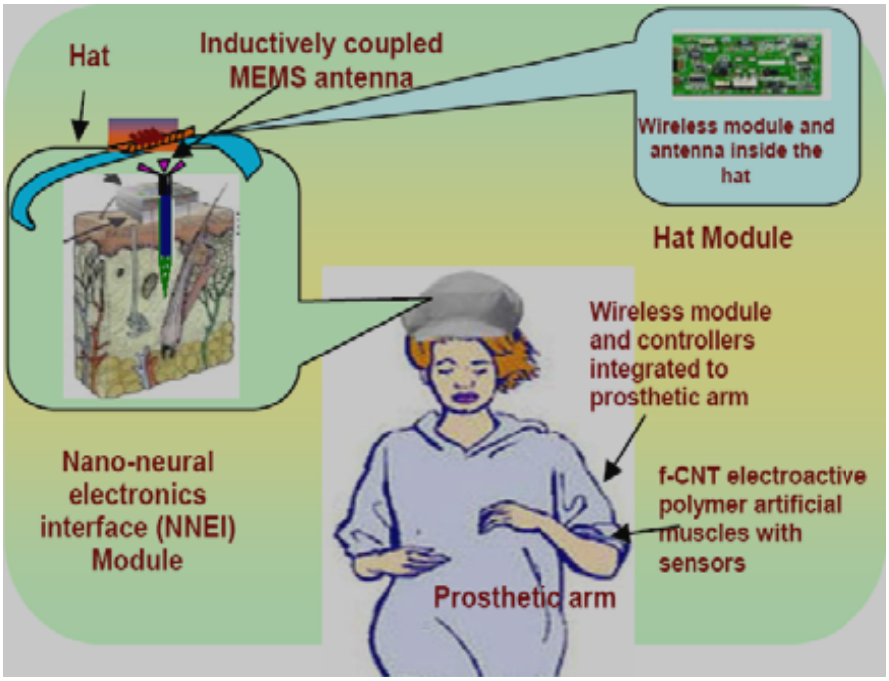

Figure 2. Implementation scheme of the wireless power and signal feed back by PPD for NEI

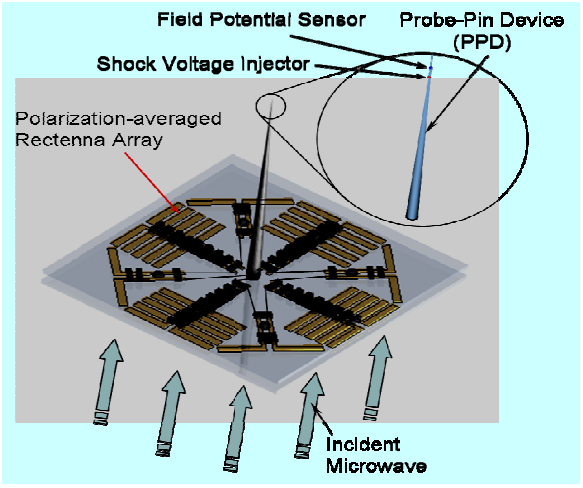

Figure 3. An array of dipole rectennas with a probe-pin device (PPD) couples with microwave to generate DC power for DBS.

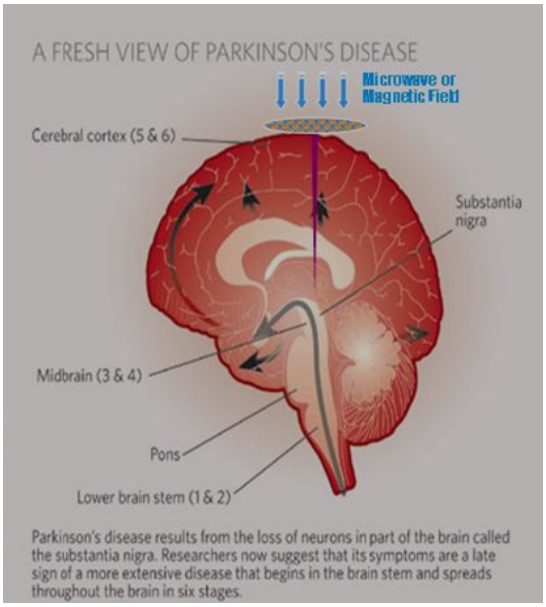

Figure 4. A wireless power receiver with a probe-pin device (PPD) is implanted for deep brain stimulation (DBS). The wireless power receiver couples with incident microwave field.

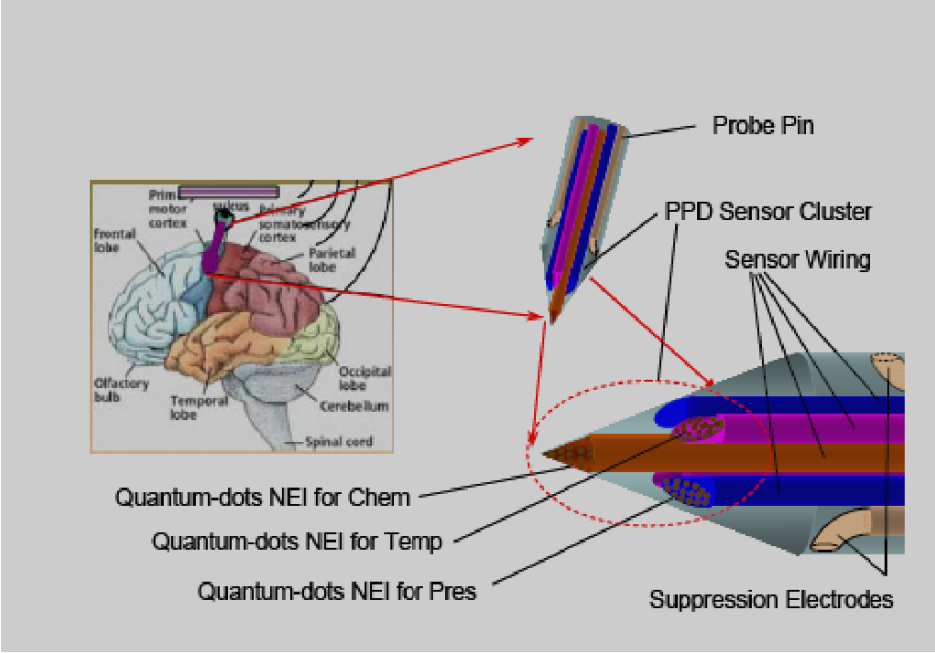

Figure 5. Schematic diagram of the NEI at the tip of PPD

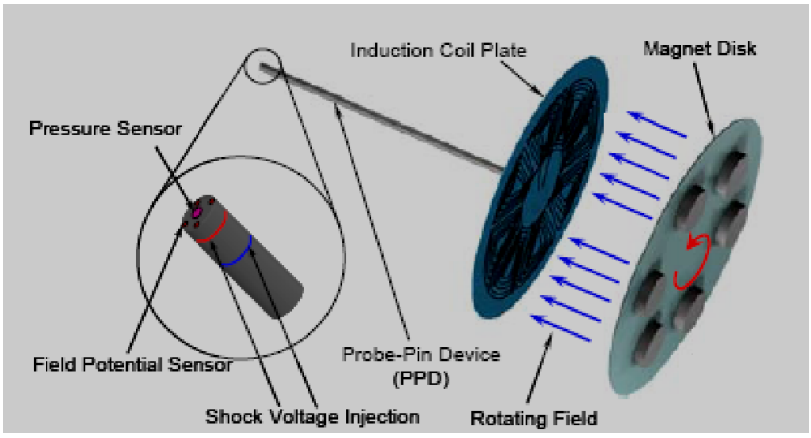

Figure 6. A magnetic induction coils with a probepin device (PPD) couples with a rotating magnetic field for DC power for DBS.

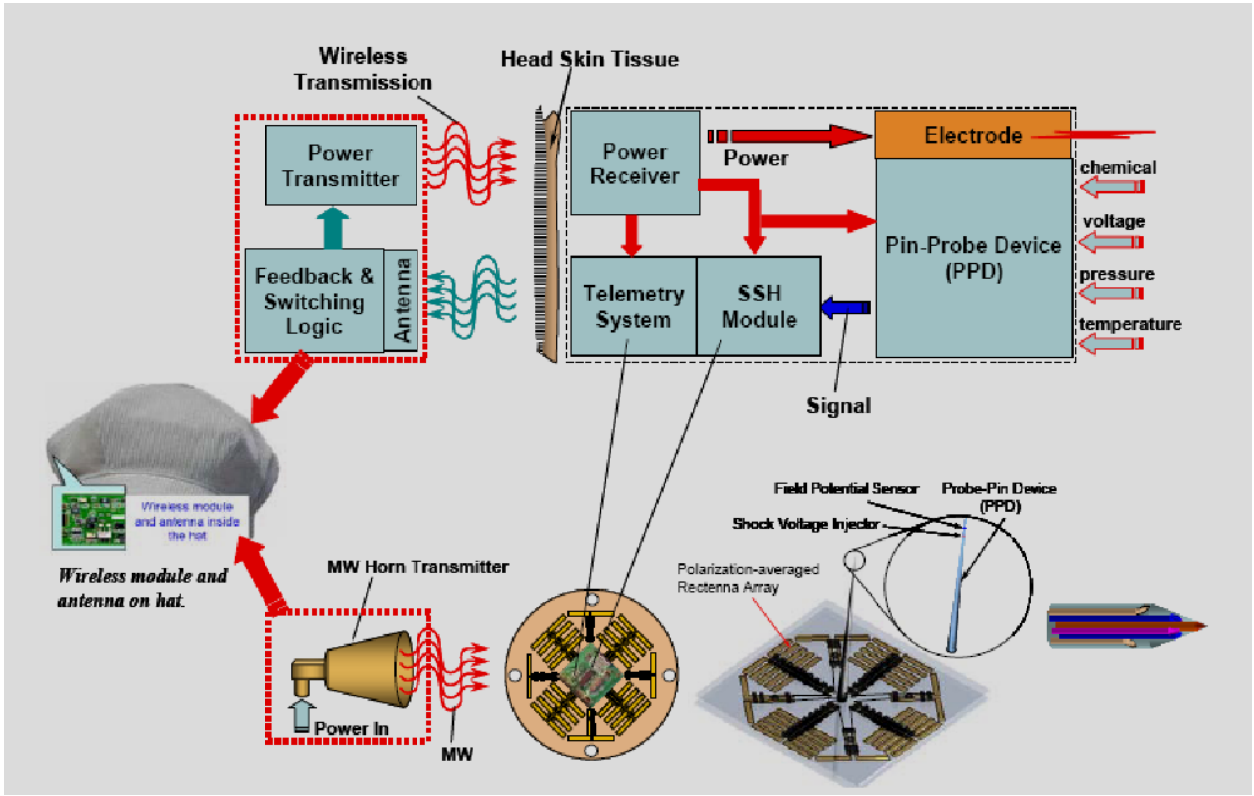

Figure 7. Schematic diagram of wireless power transmission to PPD. When rectenna array couples with incident microwave, the DC power is generated on a thin-film rectenna array plate that is placed just under head skin tissue. The power is multiplexed for feeding power for DBS and sensors at the tip of PPD.

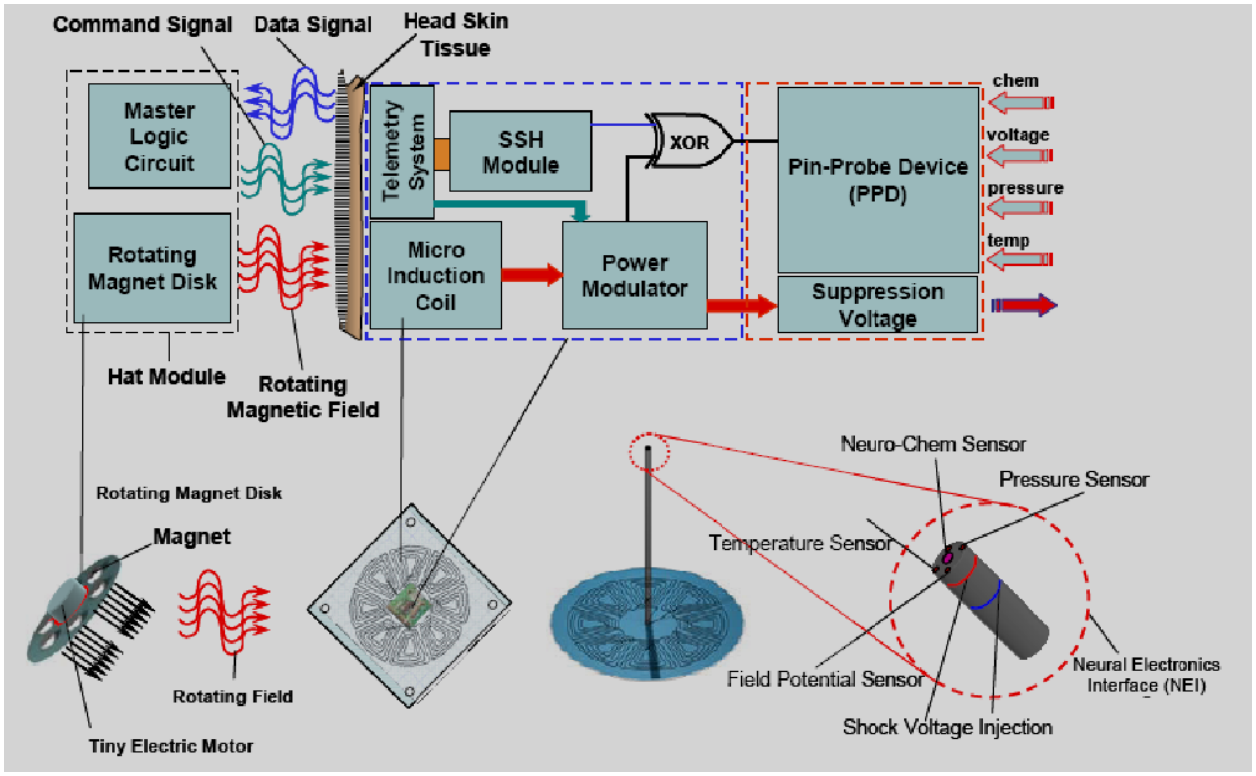

Figure 8. Schematic diagram of wireless power transmission to PPD. When rotating magnetic fluxes cut through induction coil, the power is generated on a thin-film induction coil plate that is placed just under head skin tissue. The power is multiplexed for feeding power for DBS and sensors at the tip of PPD.

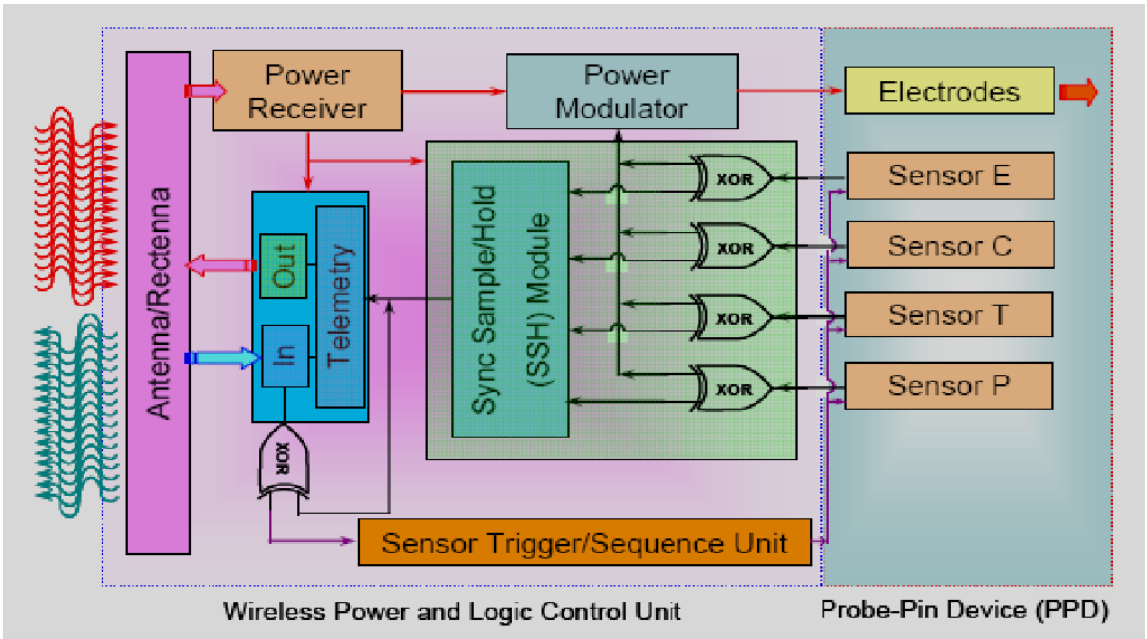

Figure 9. Wireless power and logic circuit unit using a low power microwave.

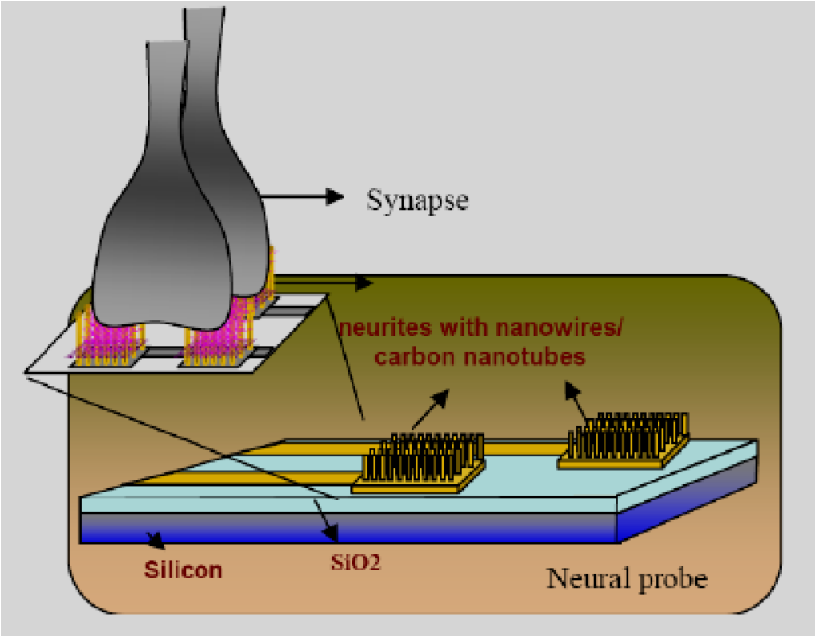

Figure 10. Schematic diagram of the neuralnanowire implant on silicon using nanowires and cultured neurites.

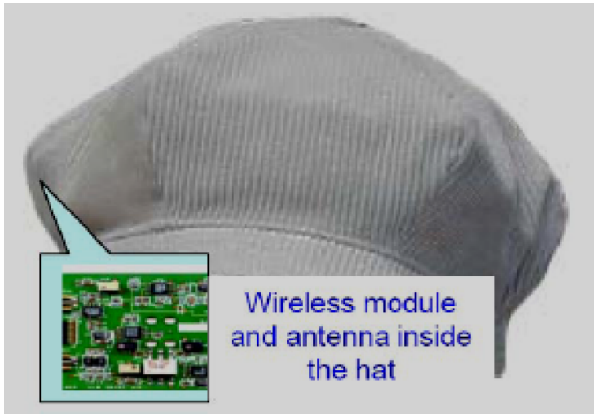

Figure 11. Wireless module and antenna on hat.

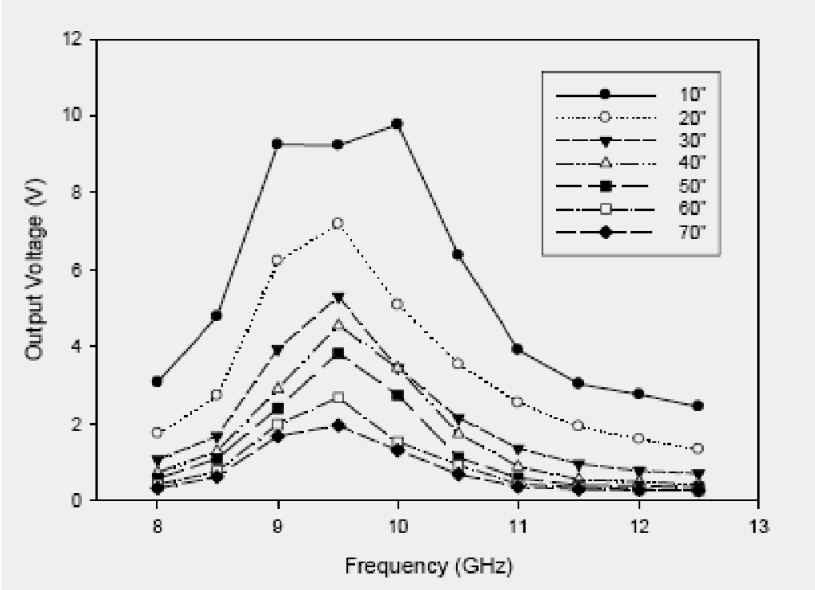

Figure 12. Output Voltage of Polyimide Rectenna vs. Distances from the Horn.

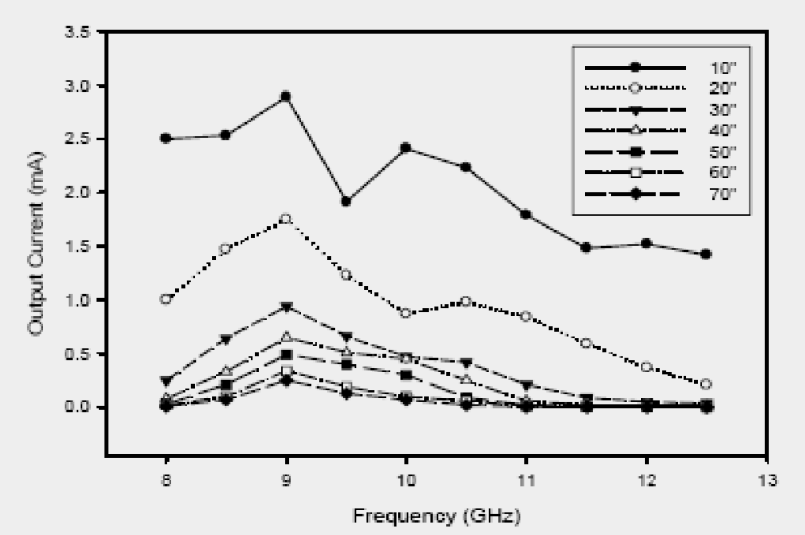

Figure 13. Output current profiles from polyimide rectenna along with distances from injection horn.

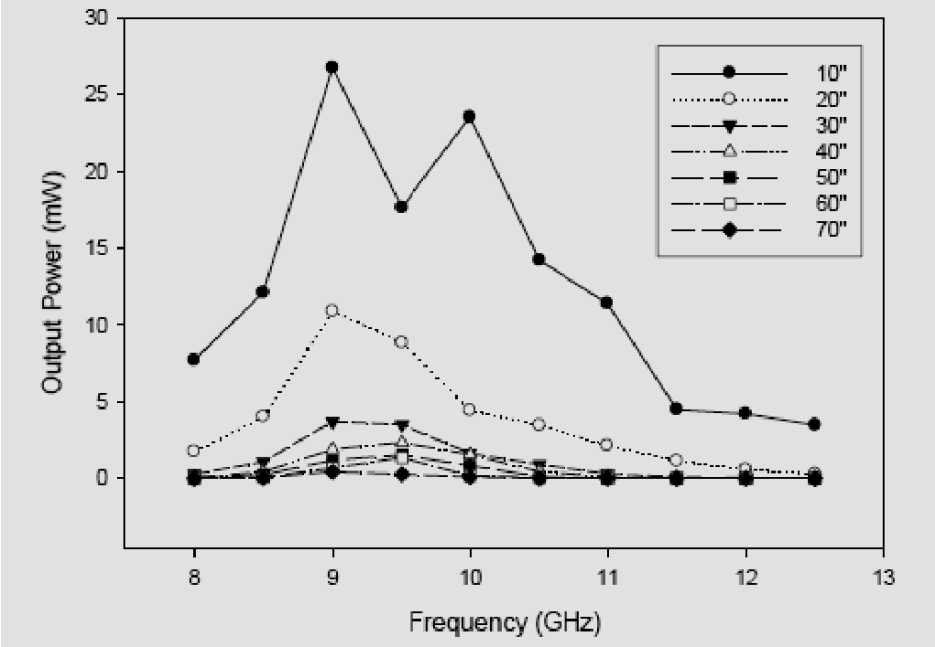

Figure 14. Output Power of Polyimide Rectenna vs. Distances.

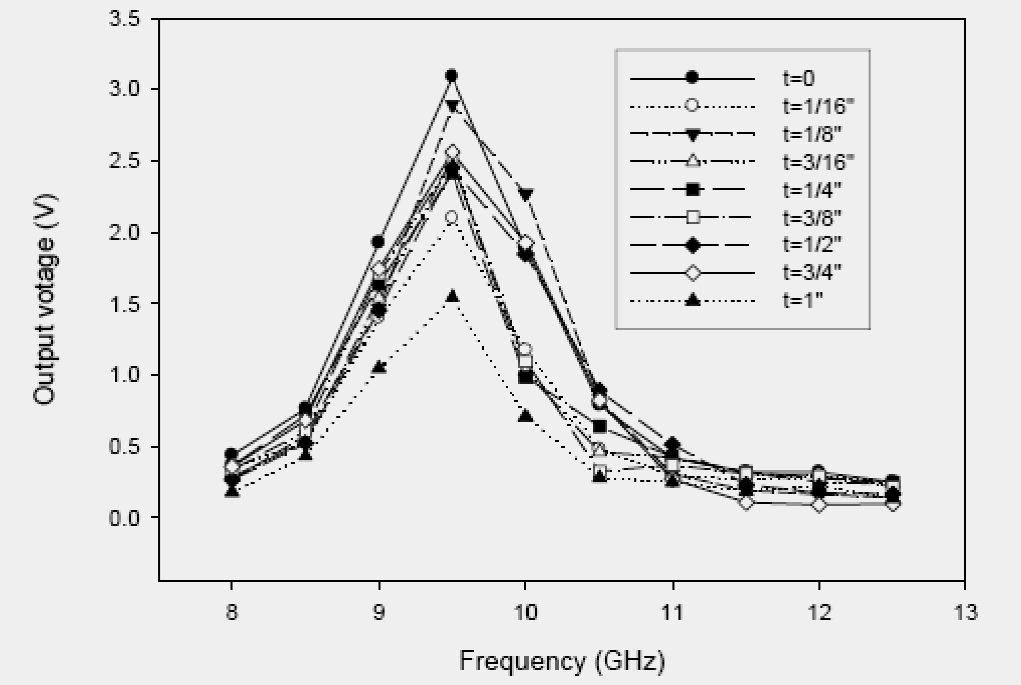

Figure 15. Output Voltage of Polyimide Rectenna through various thickness of Polyurethane at 100cm from the injection horn

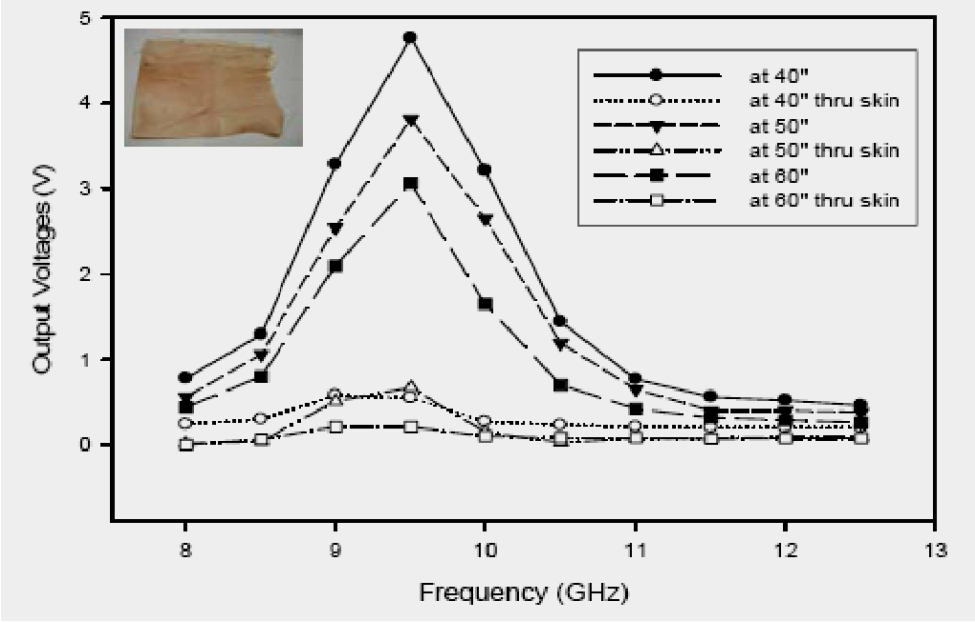

Figure 16. Output voltage captured by a rectenna array through a pig skin (1.7~2.2 mm thick).

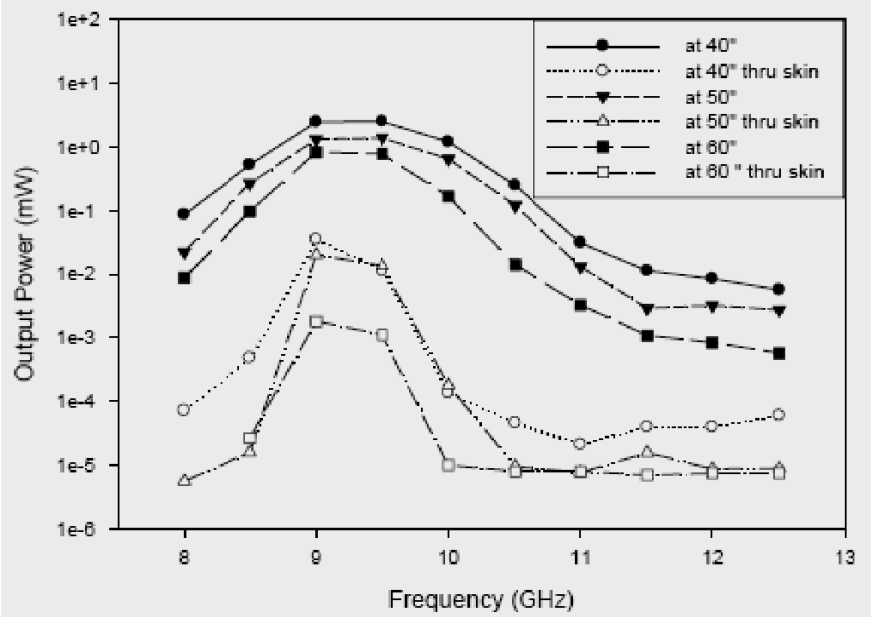

Figure 17. Output power measured by a rectenna array with and without pig skin.

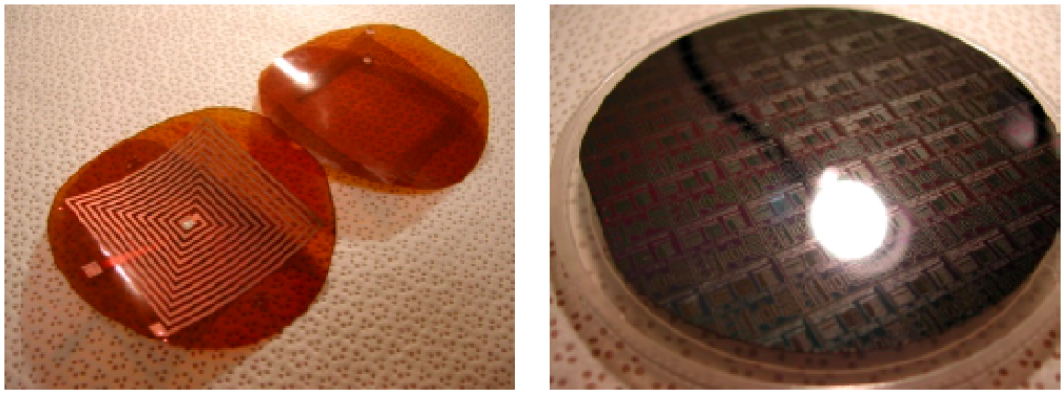

Figure 18 (a) Membrane Inductor Coil, (b) Transducer.

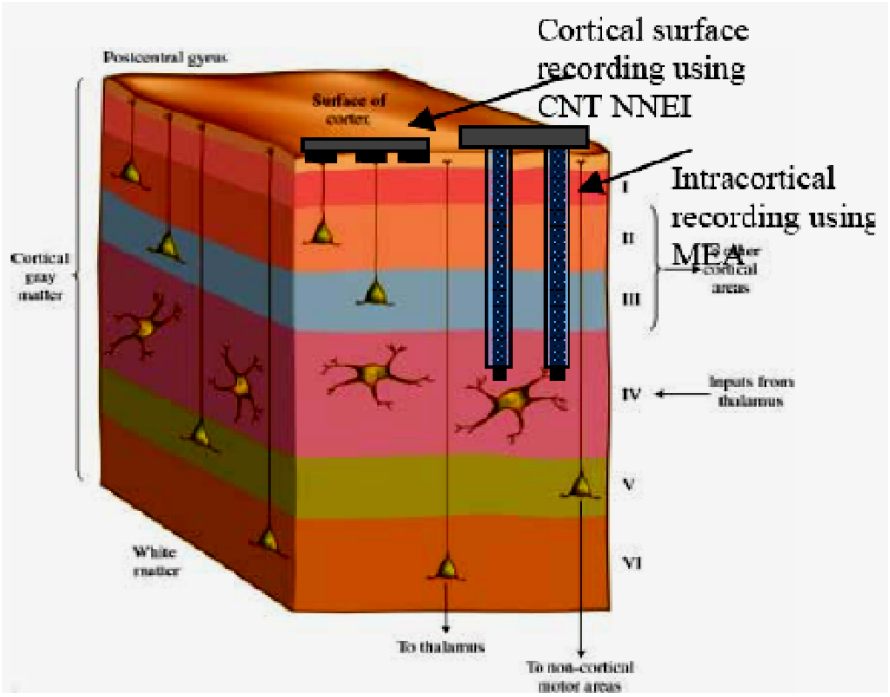

Figure 19. Schematic of the neuron architecture at the cerebral cortex and the comparison of the mechanism of cortical surface recording using QD nanoelectrode arrays vs current technologies of intracortical recording using long microelectrode arrays (MEAs). Cortex architecture is adapted from [14].

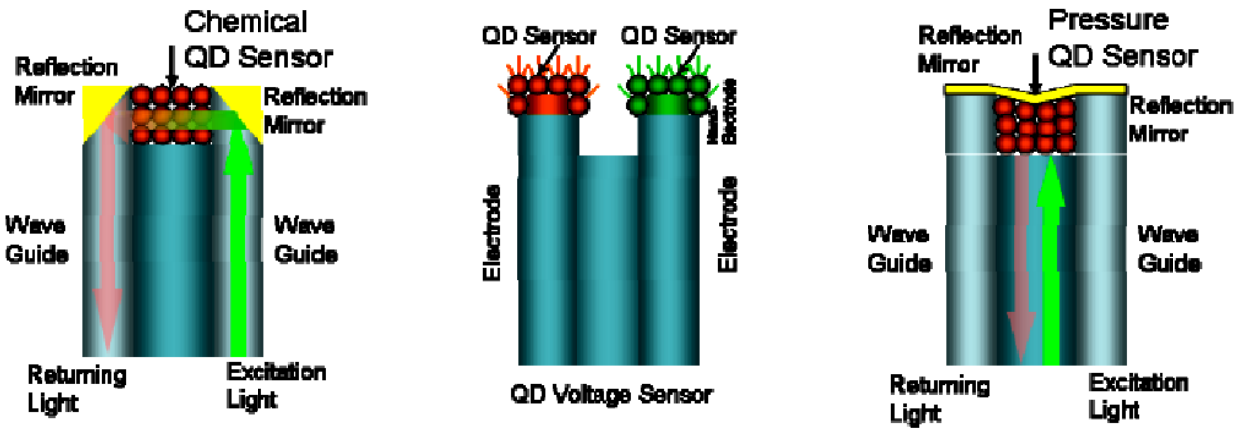

Figure 20. QD Chemical / Voltage / Pressure Sensor on PPD.

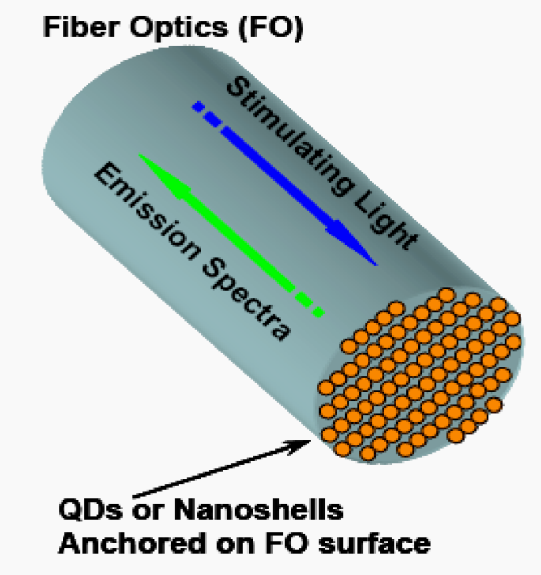

Figure 21. QD or NSs populated biosensor head.

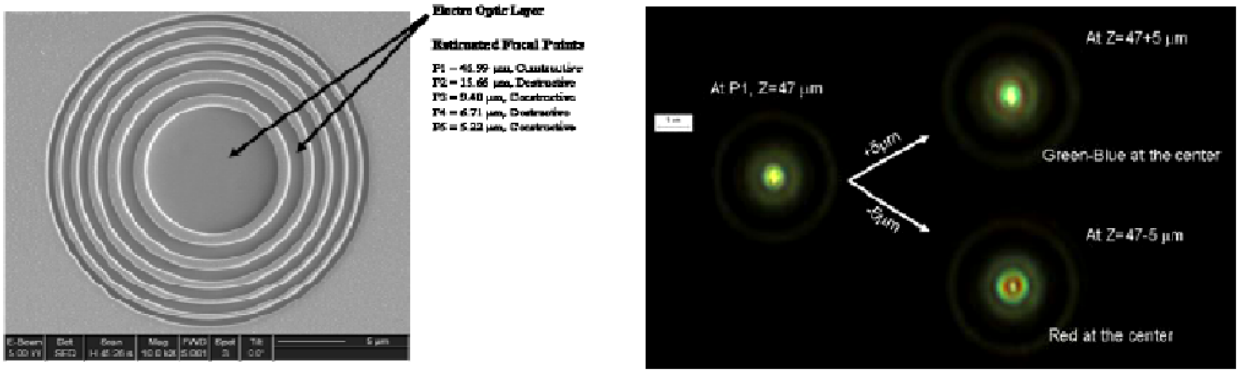

Figure 22. (Left) Fabricated zone plate as micro ring grating, (Right) Color dispersion of

micro-ring-grating near a focal point [25]

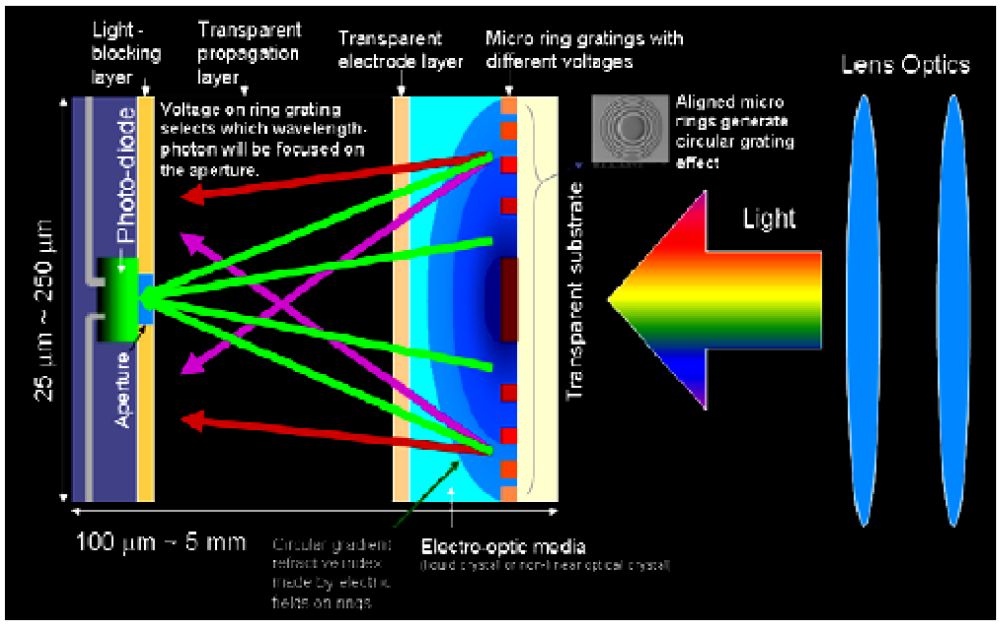

Figure 23. Design-I: Micro-ring-grating spectrometer for parallel lights. [21]

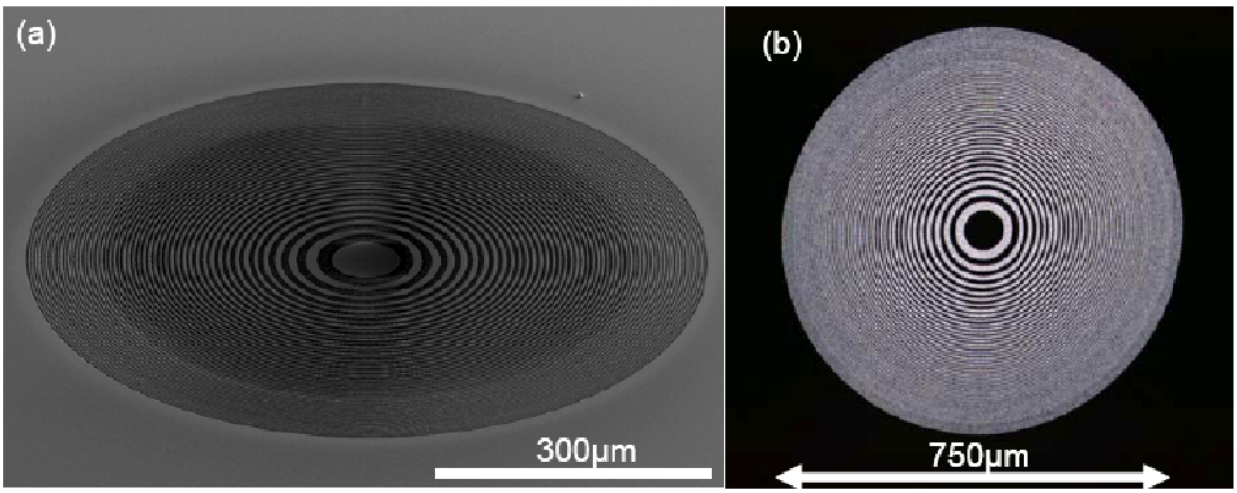

Figure 24. (a) SEM image (stage tile=52º) of half-transparent ring grating based on Zone Plate, (b) optical microscope image of the same with a light source in transmission mode.

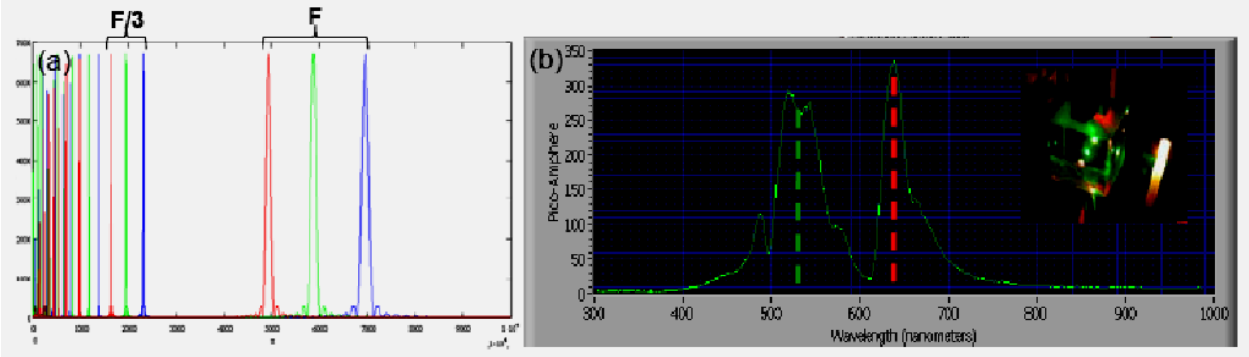

Figure 25. (a) Mathematical simulation of photon intensities with three wavelengths (red:630nm, green:532nm, blue: 450nm) on the optical axis (graph's x-axis is real optical distance Z) (b) measured micro-spectrometer spectrum (x-axis is in wavelength) from mixed yellow light(inset picture) of red (630nm) and green (532nm) lasers.

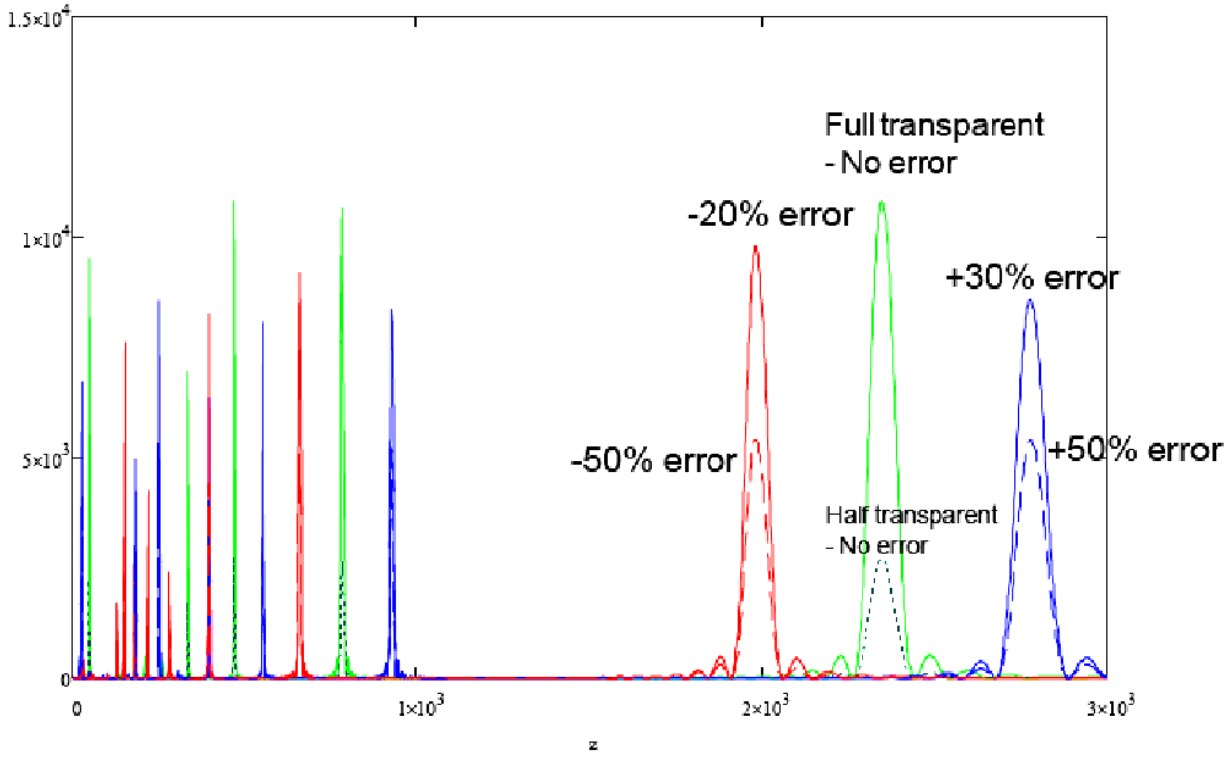

Figure 26. Photon intensity simulation on optical axis, dotted green line = half transparent grating with λ=532nm, solid green line = full transparent grating with step height difference, red and blue lines indicates 630nm and 450nm photons with various phase matching errors.

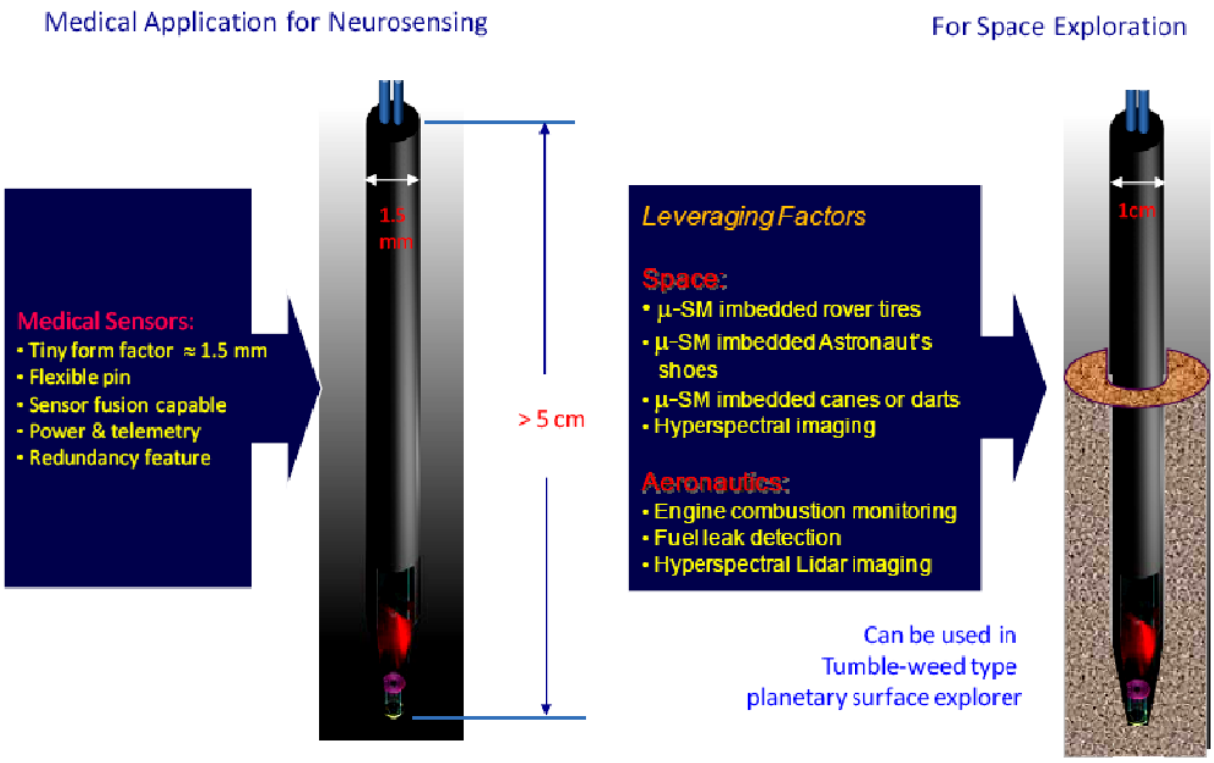

Figure 27. Generalized view of micro-spectrometer for medical and space applications.

Figure Legends

Figure 1. An electrode and batteries for DBS controlling the motor action of a PD patient.

Figure 2. Implementation scheme of the wireless power and signal feed back by PPD for NEI.

Figure 3. An array of dipole rectennas with a probe-pin device (PPD) couples with microwave to generate DC power for DBS.

Figure 4. A wireless power receiver with a probe-pin device (PPD) is implanted for deep brain stimulation (DBS). The wireless power receiver couples with incident microwave field.

Figure 5. Schematic diagram of the NEI at the tip of PPD

Figure 6. A magnetic induction coils with a probe-pin device (PPD) couples with a rotating magnetic field for DC power for DBS.

Figure 7. Schematic diagram of wireless power transmission to PPD. When rectenna array couples with incident microwave, the DC power is generated on a thin-film rectenna array plate that is placed just under head skin tissue. The power is multiplexed for feeding power for DBS and sensors at the tip of PPD.

Figure 8. Schematic diagram of wireless power transmission to PPD. When rotating magnetic fluxes cut through induction coil, the power is generated on a thin-film induction coil plate that is placed just under head skin tissue. The power is multiplexed for feeding power for DBS and sensors at the tip of PPD.

Figure 9. Wireless power and logic circuit unit using a low power microwave.

Figure 10. Schematic diagram of the neuralnanowire implant on silicon using nanowires and cultured neurites.

Figure 11. Wireless module and antenna on hat.

Figure 12. Output Voltage of Polyimide Rectenna vs. Distances from the Horn

Figure 13. Output current profiles from polyimide rectenna along with distances from injection horn.
Figure 14. Output Power of Polyimide Rectenna vs. Distances.

Figure 15. Output Voltage of Polyimide Rectenna through various thickness of Polyurethane at 100cm from the injection horn

Figure 16. Output voltage captured by a rectenna array through a pig skin (1.7~2.2 mm thick).

Figure 17. Output power measured by a rectenna array with and without pig skin.

Figure 18 (a) Membrane Inductor Coil, (b) Transducer.

Figure 19. Schematic of the neuron architecture at the cerebral cortex and the comparison of the mechanism of cortical surface recording using QD nanoelectrode arrays vs current technologies of intracortical recording using long microelectrode arrays (MEAs). Cortex architecture is adapted from [14].

Figure 20. QD Chemical / Voltage / Pressure Sensor on PPD

Figure 21. QD or NSs populated biosensor head.

Figure 22. (Left) Fabricated zone plate as micro ring grating, (Right) Color dispersion of microring-grating near a focal point [21]

Figure 23. Design-I: Micro-ring-grating spectrometer for parallel lights. [21]

Figure 24. (a) SEM image (stage tile=52º) of half-transparent ring grating based on Zone Plate, (b) optical microscope image of the same with a light source in transmission mode.

Figure 25. (a) Mathematical simulation of photon intensities with three wavelengths (red:630nm, green:532nm, blue: 450nm) on the optical axis (graph's x-axis is real optical distance Z) (b) measured micro-spectrometer spectrum (x-axis is in wavelength) from mixed yellow light(inset picture) of red (630nm) and green (532nm) lasers.

Figure 26. Photon intensity simulation on optical axis, dotted green line = half transparent grating with λ=532nm, solid green line = full transparent grating with step height difference, red and blue lines indicates 630nm and 450nm photons with various phase matching errors.

Figure 27. Generalized view of micro-spectrometer for medical and space applications.